STUDY OF THE EVOLUTION OF MICRON-SCALE PORE STRUCTURE IN OIL SHALE AT DIFFERENT TEMPERATURES

ZHIQIN KANG[*], JING ZHAO, DONG YANG, YANGSHENG ZHAO, YAOQING HU

Institute of Mining Technology, Taiyuan University of Technology, Taiyuan 030024, P. R. China

Abstract. *The micron-scale (μm) pore is the main channel of fluid percolation. The evolution of μm-sized pore structures in a cylindrical oil shale sample (φ = 0.82 × 7 mm) at different temperatures was investigated by high-precision micro-computed tomography (micro-CT) scan technology. It is found that there is a small change in pore structure when the temperature is lower than 300 °C. However, the quantity and average diameter of pores as well as porosity are all dramatically enhanced when the temperature ranges from 300 to 400 °C, and each parameter attains a maximum value when the temperature reaches 500 °C. This can be expected from the formation of a great amount of oil and gases through pyrolysis of solid organic matter at higher temperature. And so the spaces previously occupied by organic matter become the ones filled with pores.*

The newly-formed pores can be taken as the valid channels connecting the original pores. This is attested by the decrease in the quantity of pores with a diameter of 0.54–1.50 μm and the slight increase in the amount of pores having a diameter from 1.70 to 4.10 μm. Thus, the coalescence of μm-sized pores enlarged the channels facilitating the fluid percolation, in favor of the injection of heated fluids and the release of oil and gases during pyrolysis.

Keywords: micro-CT scan technology, oil shale micron-scale pore, pore structure evolution, fluid percolation.

1. Introduction

Oil shale is a type of rock which is enriched in organic matter. It is formed by the decomposition of lower-order plants, such as algae, and plankton and by anaerobic physio-chemical processes occurring at the bottom of shallow seas and lakes [1–3]. Oil shale is very sensitive to variations in temperature. A violent thermal decomposition reaction will occur inside the rock when

---

[*] Corresponding author: e-mail *kangzhiqin810101@126.com*

the temperature rises from 300 to 550 °C [4–7]. A large quantity of oil and gases can be generated by pyrolysis of solid organic matter in oil shale, involving a 10–20% weight loss. At high temperature, pores in the shale are the main conduits for the storage and percolation of oil and gases. However, the pore structure is also modified by the consumption of solid organic matter which will influence the percolation of fluids. Therefore, the rock acts as a porous medium at high temperature with a constantly evolving pore structure. The study of the evolution of pore structure at different temperatures is important for understanding the percolation and generation of oil and gases by pyrolysis. It can also serve as a guide to the development of in-situ heat injection in oil shale [8–10].

As is known, X-ray micro-computed tomography (micro-CT) has provided direct visualization and quantitative assessment of oil shale samples. In our previous work [11], the thermal cracking could be well observed and then the corresponding permeability of Fushun oil shale was expected. Moreover, Zhao et al. [12] studied the internal structure changes of Daqin and Yan'an oil shales at high temperatures. It was found that the porosity of Daqing oil shale increased from 2.23 to 31.61% and that of Yan'an oil shale from 2.70 to 8.86% when the temperature was increased from 20 to 600 °C. In addition, Saif et al. [13] investigated the dynamic imaging of Green River oil shale pyrolysis by using X-ray micro-CT with a 2 μm voxel resolution. The images reveal a dramatic change in porosity accompanying pyrolysis between 390 and 400 °C with the formation of micron-scale heterogeneous pores, which shows that the pore development is directly related to the initial spatial distribution of organic matter. Tiwari et al. [14] also studied the characteristics of oil shale pore structure before and after pyrolysis by using X-ray micro-CT with a 42 μm voxel resolution, and found that after pyrolysis the three-dimensional pore network structure with pores as large as 500 μm was developed. All this means that the method of micro-CT is valid in describing the pore structural variation since the micron-scale (μm) pore is the main channel for fluid percolation [15–17].

In this work, we study the quantity, size and connection of μm-sized pores inside the oil shale sample by the method of high-precision micro-CT scan imaging at different temperatures. The advantage of this method is its high spatial resolution, 0.54×0.54 μm. This makes the evolution of the pore structure more easily observable, and the process can be described by accurately calculating and analyzing the parameters of μm-sized pores using special CT scan imaging analysis software.

2. Sample and CT scan experimental procedures

2.1. The preparation of oil shale samples and CT testing

The experimental CT scan system is composed of a microfocus X-ray spectrometer, digital plane detector, high-precision revolving stage and

fixture, seat, horizontal movement device, and data acquisition and analysis system, as shown in Figure 1. The CT scan method is an effective tool for studying the internal structure morphology of rocks.
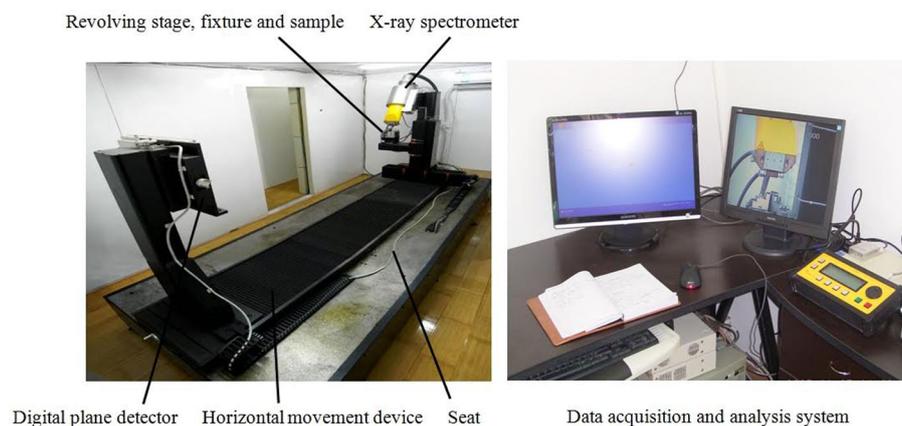

Fig. 1. Experimental micro-CT system.

The oil shale sample of dark brown color was collected from Fushun in Liaoning Province, China. The results of Fischer Assay analysis of Fushun oil shale are presented in Table 1 showing its oil content to be 8.20%. The thermogravimetric (TG) curve of the sample as a function of temperature at a heating rate of 15 °C/min is depicted in Figure 2. From the figure it is clear that there are three significant stages of weight loss. In the first stage when the temperature is below 200 °C, the disappearance of evaporation of water occurs. In the second stage the temperature ranges from 330 to 550 °C. In this stage the actual pyrolysis process of organic matter takes place. This is evident from the weight loss curve falling sharply when the temperature rises from 350 to 480 °C. The final stage (above 550 °C) is characterized by the dissociation of clay and carbonate minerals.

The test sample was of cylindrical shape ($\varphi = 0.82 \times 7$ mm). During the CT experiment, the sample was installed vertically at the center of the micro-CT scanning system revolving stage to guarantee maximum magnification (Fig. 3). A CT scan was first performed at room temperature. Then the sample was put into a high temperature oven for heating in an oxygen-free environment. The temperature was increased to 100 °C during 30 min and

Table 1. Fischer Assay analysis of Fushun oil shale, wt%

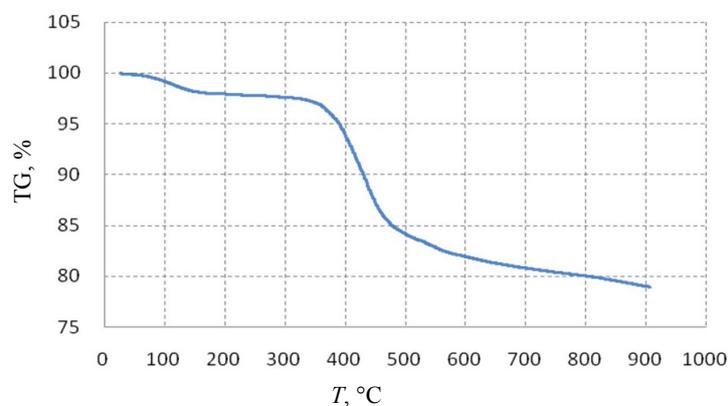| Sample	Water	Residue	Oil	Gas and loss
Fushun oil shale	5.00	83.22	8.20	3.58

Fig. 2. TG curve of the Fushun oil shale sample at a heating rate of 15 °C/min.

Fig. 3. The cylinder-shaped sample of oil shale ($\varphi = 0.82 \times 7$ mm).

the heat power turned off to let the sample cool to room temperature in the oven. Thereafter the oil shale sample was taken out and placed on the revolving stage for CT scanning. Following the same fashion, the experimental temperatures were increased at 100 °C intervals up to a maximum temperature of 600 °C.

2.2. CT scan grayscale images and binarization processing

Figure 4 shows the micro-CT scan grayscale images of the oil shale sample at different temperatures and in different horizontal positions. The resolution was set at 0.54×0.54 μm. The image coloring changed continuously from black to gray to white, marking differences in density. In the figure, white color represents high density mineral grains, black color symbolizes pore spaces, whereas the gray regions correspond to low density clay minerals and organic matter occupying the largest area. Since it is difficult to resolve

small variations in the grayscale tone under the microscope, the micro-CT scan grayscale images were processed by binarization to extract the pores and reveal the evolution of μm-sized pore structure.

The binarization processing also concerns the image segmentation. The binarization could make the solid frame and pores remain, so that the quantity, shape and size of and connection between the pores can be directly observed. The process of binarization is to compare the gray value of each grayscale pixel of the obtained images with the gray value of air. The corresponding pixels are divided into two types: (1) the pixel gray value which is higher than that of air is taken to be 1, representing the solid frame in the image; (2) the pixel gray value being lower than or equal to that of air is referred to as 0, corresponding to the pores in the image. As is known, the binarization processing equation of grayscale images can be expressed by:

$$f(x,y) = \begin{cases} 1 & f(x,y) > \theta \\ 0 & f(x,y) \le \theta, \end{cases} \tag{1}$$

where $f(x, y)$ is the gray value of each pixel having an (x, y) coordinate and θ is the gray value of air which is equal to 0.0021 in our experiment.

The largest square within a 900×900 pixels area of a grayscale image of the oil shale sample was selected for binarization processing (Fig. 4). This square contained a total of 81×10^4 pixels and covered an area of 0.49×0.49 mm^2. For each temperature test point, 20 grayscale images set in different horizontal positions were treated by binarization. In total, 140 binarization images were selected to extract the pore structure parameters to create a database.
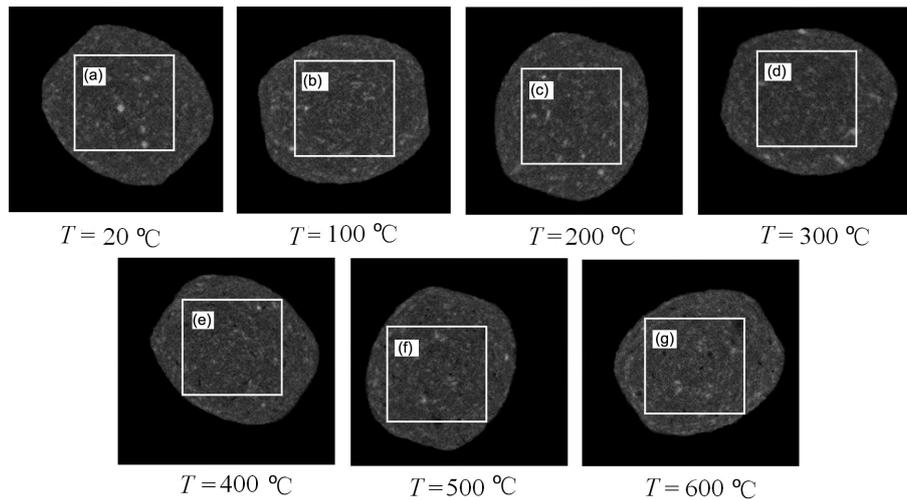

Fig. 4. CT scan grayscale images of the oil shale sample at different temperatures.

Figure 5 depicts the μm-sized pore structure of the oil shale sample obtained after the binarization processing at different temperatures, the square regions of (a), (b), (c), (d), (e), (f) and (g) corresponding to the respective temperatures in Figure 4. The white zones in Figure 5 correspond to the rock frame, whereas the color zones relate to pores. The smallest pore diameter is 0.54 μm, corresponding to the size of one pixel. The μm-sized pore structures were widely developed throughout the oil shale sample. The pores had various forms, from angular and circular to dendritic, and their structure was modified with increasing temperature.
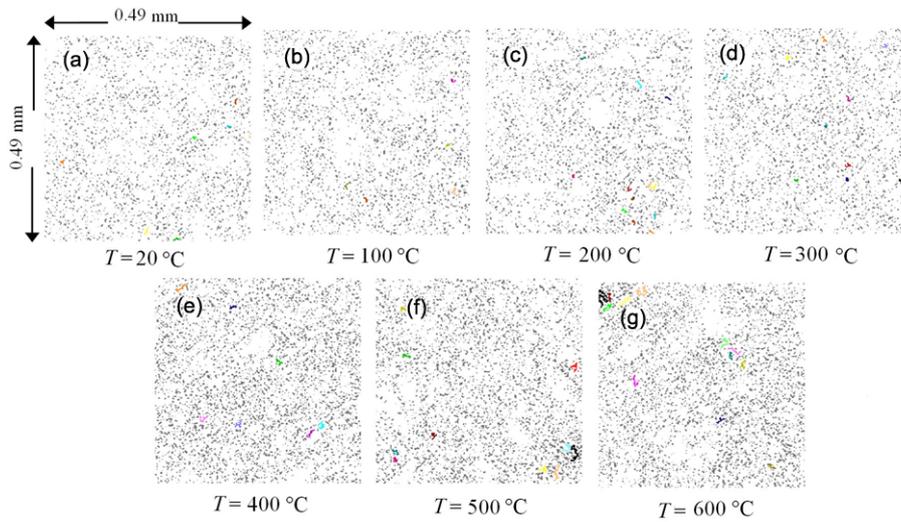

Fig. 5. The μm-sized pore structure of the oil shale sample obtained after binarization at different temperatures.

2.3. Treatment by equivalent circular pores

Since the pore structure of the oil shale sample is irregular, the statistical analysis was not conducted using a unified standard. So, pores of various shapes can be treated as circular pores for simplification. For each pore, the equivalent pore diameter can be calculated according to the following equation:

$$d = 2\sqrt{\frac{n \cdot A}{\pi}}, \qquad (2)$$

where d is the equivalent pore diameter; n is the number of pixels in each irregular pore and A is the area of each pixel point, in this case $A = 0.54 \times 0.54$ μm^2.

3. Evolution of μm-sized pore structure in the oil shale sample at different temperatures

3.1. Change of μm-sized pore structure parameters with temperature

Special CT scan image analysis software was used for calculations. The pore structure parameters of the square regions (Fig. 5a–g) are presented in Table 2. Figures 6 and 7, which were drawn based on the data given in Table 2, illustrate the relationship of the quantity, total area and average diameter of pores as well as porosity with temperature. The figures reveal no significant change or only small fluctuations in these parameters at temperatures from 20 to 300 °C. However, between 300 and 400 °C all these parameters are strongly increased, and reach maximum values when 500 °C is attained. The average pore diameter and porosity increase from 1.516 to 1.727 μm and from 7.95 to 12.51%, respectively. Though, there is a slight

Table 2. Pore structure parameters of the oil shale sample at different temperatures

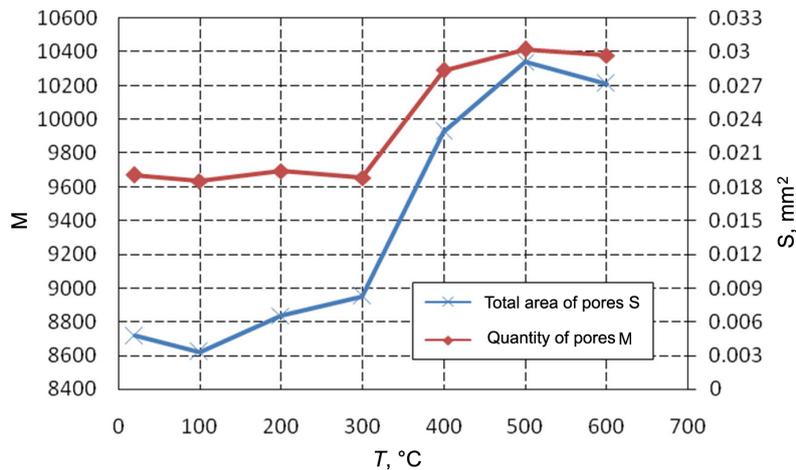| Temperature T, °C	Square region	Quantity of pores M	Total area of pores S, mm^2	Average pore diameter d, μm	Porosity n, %
20	(a)	8716	0.019055	1.516	7.95
100	(b)	8622	0.018519	1.504	8.26
200	(c)	8836	0.019403	1.518	8.1
300	(d)	8952	0.018792	1.524	7.73
400	(e)	9929	0.028337	1.702	11.75
500	(f)	10340	0.030220	1.727	12.51
600	(g)	10212	0.029696	1.719	12.29

Fig. 6. Variations in the quantity and total area of pores in the oil shale sample with temperature.
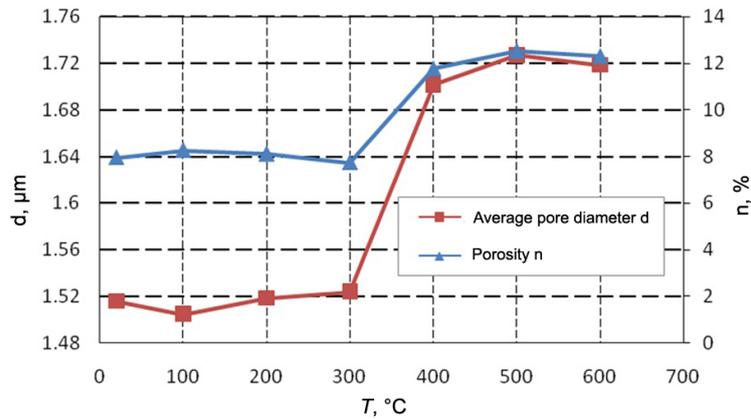
Fig. 7. Variations in the average pore diameter and porosity of the oil shale sample with temperature.

decrease in the two parameters when the temperature exceeds 500 °C. It should be mentioned that there will be an abrupt variation in the μm-sized pore structure when the temperature is between 300 and 400 °C.

Figure 8 illustrates the variations in the proportion of μm-sized pores with pore diameter at different temperatures. The diameter of μm-sized
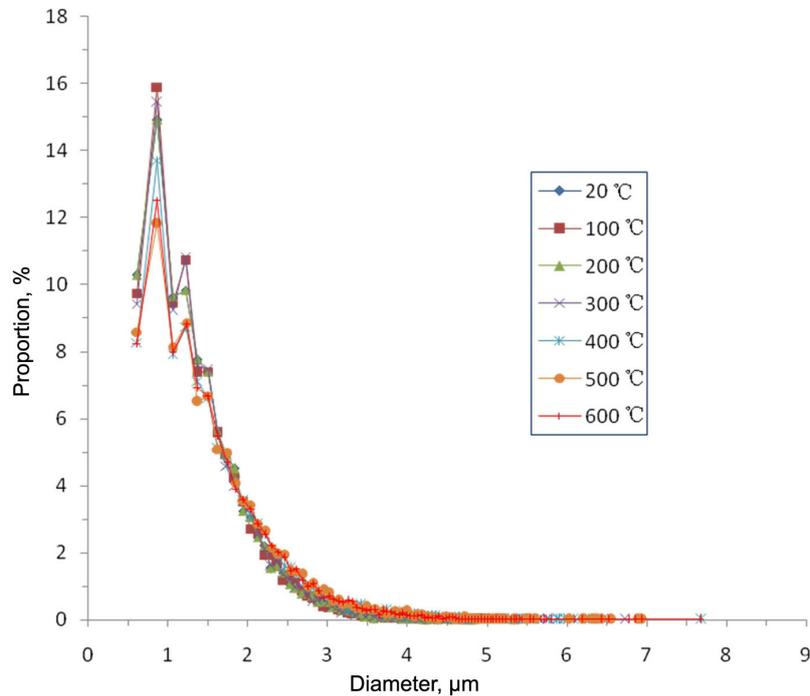

Fig. 8. Variations in the proportion of μm-sized pores in the oil shale sample with pore diameter at different temperatures.

pores ranges from 0.54 to 7.80 μm. This proportion first increases and then decreases with increasing pore diameter. Thus, there is a maximum proportion of pores when the diameter is 0.85 μm. However, elevating the temperature caused a series of complicated physical and chemical changes within the oil shale sample, which will influence the distribution of μm-sized pores. When increasing the temperature from 20 to 600 °C, the proportion of pores with a diameter of 0.54–1.50 μm decreases, while the decrease is especially noticeable when the temperature ranges from 300 to 600 °C.

The proportion of pores having a diameter from 0.54 to 1.50 μm decreases about 3.0% at 600 °C, while that of pores with a diameter of 1.70–4.10 μm increases slightly (about 0.80% increase). This implies that there exists a connection between several small pores with a diameter of 0.54–1.50 μm at high temperature, leading to the formation of large pores having a diameter from 1.70 to 4.10 μm.

A 3D reconstruction of several planar CT scan grayscale images was performed according to the sequence to obtain actual volumes of $0.22 \times 0.22 \times 0.22$ mm^3 of the oil shale sample at different temperatures (Fig. 9a). The 3D grayscale images were then treated by binarization to segment the rock frame and pores. The largest pore cluster was later extracted from numerous pores as shown in Figure 9b. It was found that the size of the largest pore cluster at 20 °C was relatively small, being limited to 5.27×10^3 μm^3. So, all μm-sized pores were probably small at room temperature and insulated,
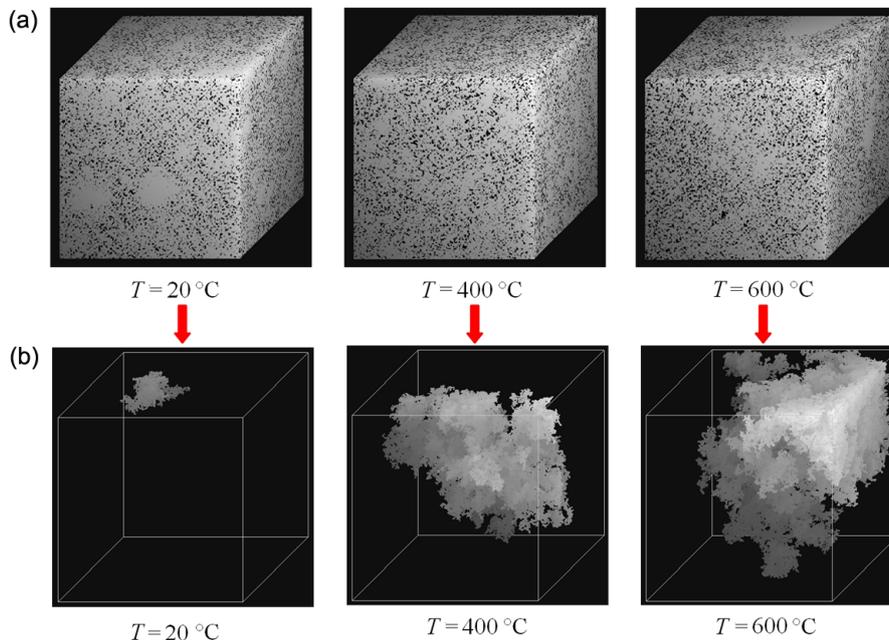

Fig. 9. (a) 3D grayscale images of the oil shale sample ($0.22 \times 0.22 \times 0.22$ mm^3); (b) the largest pore cluster at different temperatures.

resulting in low permeability throughout the oil shale sample. However, the pores will be interconnected when the temperature increases gradually, resulting in a substantial increase in the size of the pore cluster with a thin "snow-shaped" layered morphology. It can be seen that the largest pore clusters have the volumes of 122.59×10^3 and 297.72×10^3 μm^3 at 300 and 600 °C, respectively. This is 20–50 times the pore volume obtained at room temperature. So, it is clear that oil shale exhibits good permeability at high temperature. As is evident from Figures 5 and 9b, the coalescence of μm-sized pores at high temperature was better to be seen by 3D imaging than by 2D imaging. Thus, the injection of heated fluids and the release of oil and gases during pyrolysis become easier, due to the expanded channels of fluid percolation.

3.2. Analysis of the evolution of μm-sized pore structure

The change in the μm-sized pore structure of oil shale reflects the modification of its internal structure. Since oil shale contains a large amount of organic matter, a series of complicated physical and chemical changes inevitably occur in its internal structure especially at high temperature, leading to the variation of the μm-sized pore structure.

3.2.1. Temperature range of 20–300 °C

The physical changes in the studied oil shale sample mainly occurred when the temperature ranged from 20 to 300 °C. Firstly, the water in the sample was evaporated with temperature increase (Fig. 2). Second, the formation of the stress concentration due to the anisotropy of thermal expansion of rock particles was inevitable, resulting in thermal cracking. In addition, the compressive deformation of the existing pores could happen because of the influence of high temperature on solid organic matter. On account of all these effects, there were some fluctuations in parameters, such as the quantity and diameter of pores as well as rock porosity, while the pore structure underwent a small change on a μm scale.

3.2.2. Temperature range of 300–500 °C

When the temperature exceeded 300 °C, a rapid pyrolysis of organic matter occurred and oil and hydrocarbon gases were generated, the fluids volume being several hundred times the volume of original organic matter. Several pores of different size were formed in the space previously occupied by organic matter. This explains why the quantity of pores rapidly increased, the average pore diameter became larger and even the porosity was enhanced in this temperature range. Then, the volume of shale oil and hydrocarbon gases considerably increased during heating, followed by the ejecting of the latter with high velocity. So, the expansion pressure in pores made them become larger and larger, resulting in the formation of a new pore space of relatively large volume. Moreover, several thin pore walls broke up, which

led to the interconnection of small pores forming larger pores. This can explain why the proportion of pores with a diameter of 0.54–1.50 μm was decreased and that of pores having a diameter of 1.70–4.10 μm increased. Thus, we can say that the chemical reaction of organic matter with temperature rising from 300 to 500 °C will induce and drive the evolution of μm-sized pore structure in oil shale.

3.2.3. Temperature range of 500–600 °C

As seen from Figure 2, when the temperature rises from 500 to 600 °C, some organic matter remaining from pyrolysis produces a small amount of oil and gas, which almost have no role in the expansion of pores volume. So, the fluids could be freely released through the previously-formed channels. Decomposition of carbonates in oil shale begins in the temperature region of 500–600 °C. In this process some fixed carbon undergoes coking carbonization [1, 18–20]. Then there may take place the fragmentation of the rock and even the collapse of some pore walls, leading to the inhibition of pores formation.

4. Conclusions

The characteristics and evolution of the μm-sized pore structure of a cylindrical-shaped oil shale sample were systematically analyzed and studied by means of high-precision micro-CT scan technology. The experiments were carried out at temperatures from 20 to 600 °C. Based on the results obtained the following conclusions can be drawn:

1. The quantity and average diameter of pores as well as porosity increase dramatically when the temperature rises from 300 to 400 °C, and each parameter attains a maximum value when the temperature reaches 500 °C.
2. The proportion of pores with a diameter of 0.54–1.50 μm is higher, being maximum when the pore diameter is 0.85 μm, at any temperature studied. With the temperature increasing from 20 to 600 °C, the quantity of pores with a diameter of 1.70– 4.10 μm increases since the pores connect with small ones having a diameter of 0.54–1.50 μm.
3. A thin "snow-shaped" layered morphology of the largest pore clusters is observed, which can be well described by 3D modeling. Moreover, the volume of the largest pore cluster increases with increasing temperature.
4. Pyrolysis of solid organic matter occurring in the temperature range of 300–500 °C is the main factor controlling the evolution of μm-sized pore structure.

Acknowledgments

REFERENCES

1. Qian, J. L., Yin, L., Li, S. Y. *Oil Shale – Petroleum Alternative*. China Petrochemical Press, Beijing, 2010.
2. Li, S. Y., Ma, Y., Qian, J. L. Global oil shale research, development and utilization today and an overview of three oil shale symposiums in 2011. *Sino-Global Energy*, 2012, **17**(2), 8–17 (in Chinese).
3. Dyni, J. R. Geology and resources of some world oil-shale deposits. *Oil Shale*, 2003, **20**(3), 193–252.
4. Li, S. Y., Yue, C. T. Study of pyrolysis kinetics of oil shale. *Fuel*, 2003, **82**(3), 337–342.
5. Li, S. Y., Yue, C. T. Study of different kinetic models for oil shale pyrolysis. *Fuel Process. Technol.*, 2004, **85**(1), 51–61.
6. El harfi, K., Mokhlisse, A., Chanaa, M. B., Outzourhit, A. Pyrolysis of Moroccan (Tarfaya) oil shales under microwave irradiation. *Fuel*, 2000, **79**(7), 733–742.
7. Razvigorova, M., Budinova, T., Petrova, B., Tsyntsarski, B., Kinci, E., Ferhat, M. F. Steam pyrolysis of Bulgarian oil shale kerogen. *Oil Shale*, 2008, **25**(1), 27–36.
8. Kök, M. V., Guner, G., Bagci, S. Laboratory steam injection applications for oil shale fields of Turkey. *Oil Shale*, 2008, **25**(1), 37–46.
9. Kang, Z. Q., Lu, Z. X., Yang, D., Zhao, Y. S. The solid-fluid-thermal-chemistry coupling mathematical model for oil shale in-situ steam injecting development. *Journal of Xian Shiyou University*, 2008, **23**(4), 30–34 (in Chinese).
10. Zheng, D. W., Li, S. Y., Ma, G. L., Wang, H. Y. Autoclave pyrolysis experiments of Chinese Liushuhe oil shale to simulate in-situ underground thermal conversion. *Oil Shale*, 2012, **29**(2), 103–114.
11. Kang, Z. Q., Yang, D., Zhao, Y. S., Hu, Y. Q. Thermal cracking and corresponding permeability of Fushun oil shale. *Oil Shale*, 2011, **28**(2), 273–283.
12. Zhao, J., Yang, D., Kang, Z. Q., Feng, Z. C. A micro-CT study of changes in the internal structure of Daqing and Yan'an oil shales at high temperatures. *Oil Shale*, 2012, **29**(4), 357–367.
13. Saif, T., Lin, Q. Y., Singh, K., Bijeljic, B., Blunt, M. Dynamic imaging of oil shale pyrolysis using synchrotron X-ray microtomography. *Geophys. Res. Lett.*, 2016, **43**(13), 6799–6807.
14. Tiwari, P., Deo, M., Lin, C. L., Miller, J. D. Characterization of oil shale pore structure before and after pyrolysis by using X-ray micro CT. *Fuel*, 2013, **107**, 547–554.
15. Sun, L. N., Tuo, J. C., Zhang, M. F., Wu, C. J., Wang, Z. X., Zheng, Y. W. Formation and development of the pore structure in Chang 7 member oil-shale

from Ordos Basin during organic matter evolution induced by hydrous pyrolysis. *Fuel*, 2013, **158**, 549–557.

16. Clarkson, C. R.,   Solano, N.,   Bustin, R. M.,   Bustin. A. M. M.,   Chalmers, G. R. L., He, L., Melnichenko, Y. B., Radinski, A. P., Blach, T. P. Pore structure characterization of North American shale gas reservoirs using USANS/SANS, gas adsorption, and mercury intrusion. *Fuel*, 2013, **103**, 606–616.

17. Han, X. X., Jiang, X. M., Yu, L. J., Cui, Z. G. Change of pore structure of oil shale particles during combustion. Part 1. Evolution mechanism. *Energ. Fuels*, 2006, **20**(6), 2408–2412.

18. Sedman, A., Talviste, P., Kirsimäe, K. The study of hydration and carbonation reactions and corresponding changes in the physical properties of co-deposited oil shale ash and semicoke wastes in a small-scale field experiment. *Oil Shale*, 2012, **29**(3), 279–294.

19. Mõtlep, R., Kirsimäe, K., Talviste, P., Puura, E., Jürgenson, J. Mineral composition of Estonian oil shale semi-coke sediments. *Oil Shale*, 2007, **24**(3), 405–422.

20. Shi, Y. Y., Li, S. Y., Ma, Y., Yue, C. T., Shang, W. Z., Hu, H. Q., He, J. L. Pyrolysis of Yaojie oil shale in a Sanjiang-type pilot-scale retort. *Oil Shale*, 2012, **29**(4), 368–375.